Int. J. Electrochem. Sci., 13 **(2018)** 12226 – 12237, doi: 10.20964/2018.12.63

International Journal of
ELECTROCHEMICAL
SCIENCE
www.electrochemsci.org

Pd Nanoparticles Anchored on N-rich Graphdiyne Surface for Enhanced Catalysis for Alkaline Electrolyte Oxygen Reduction

Yanrong Li[1†], Yao Liu[2†], Zhongbin Li[2], Jiaqiang Li[3], Chaozhong Guo[2,*], Jin Zhang[1,2], Jinbiao Wang[2,*]*

[1] College of Materials Sciences and Engineering, Chongqing University of Technology, Chongqing 400054, P. R. China.
[2] Research Institute for New Materials Technology, School of Chemistry and Chemical Engineering, Engineering Research Center of New Energy Storage Devices and Applications, Chongqing University of Arts and Sciences, Chongqing 402160, P. R. China.
[3] School of Chemistry and Chemical Engineering, Chongqing University, Chongqing 401331, P. R. China.
[*]E-mail: guochaozhong1987@163.com
[†]*These authors equally contributed to this work, and they are the co-first author.*

Received: 28 August 2018 / *Accepted:* 30 September 2018 / *Published:* 5 November 2018

Graphdiyne (GDY) as a novel allotrope has been theoretically predicted to be the most stable non-natural carbon allotropes. However, GDY has not been systematically investigated as a new carbon support to ORR catalysts. Thus, here we report a new strategy for the synthesis of Pd nanoparticles anchored on nitrogen-doped graphdiyne (CN_x-Pd@GDY) electrocatalyst for oxygen reduction reaction (ORR) *via* a facile pyrolysis method. The results show that the prepared CN_x-Pd@GDY catalyst has exhibited excellent ORR catalysis performance with a four-electron transfer pathway in 0.1 mol l^{-1} KOH electrolyte compared to other commercial carbon supports such as carbon black and carbon nanotubes. Electrochemical research results show that the as-formed CN_x-Pd@GDY exhibits excellent electrocatalytic ORR activity with an onset potential of 0.96 V *vs.* RHE and a high long-term stability in the alkaline condition. The interaction between Pd nanocrystals and the encapsulating PANI shells was found in the catalyst, which markedly contributes to the improvement in ORR catalytic activity and stability of the catalyst. Such catalytic characteristics have reasonably indicated a great potential as a novel catalyst for ORR instead of the commercial Pt-based catalyst.

Keywords: N-rich Graphdiyne, Electrocatalyst, Oxygen reduction reaction

1. INTRODUCTION

During the past decades, a lot of scientists have developed several synthesis methods in the study of electrocatalysts for fuel cells, which endow power sources with environmentally friendly and expand their application in mobile and stationary. In the preliminary stage, it is a significant importance for fuel

cells to develop a promising catalyst for the oxygen reduction reaction (ORR) [1-4]. So far, as a member of the catalysts, the Pt metals on a carbon support (Pt/C) is still considered as the most efficient catalysts for ORR [5, 6]. The electrochemical activity and utilization can be increased by dispersedly supporting Pt nanoparticles on nanoscaled porous carbon surface, but can effectively promote the overall cost of fuel cells [7-9]. However, the long-term operation of proton exchange membrane fuel cells is still highly desired because the stability of the Pt/C catalyst for ORR cannot meet the practical requirements in the future.

Graphdiyne (GDY), one among the variety of carbon materials, possesses of large conjugated system, wide surface spacing and highly chemical stability, and tends to be similar to grapheme with the characteristics of monolayer two-dimensional planar materials. It is extensively studied in various applications in the past ten years [10-13]. At present, GDY owns a wide range of promising applications in photocatalytic degradation [14], lithium storage [15], supercapacitor [16], ultraviolet photodetector [17], and oil/water separation [18]. More recently, the functionalization of GDY with metal-Fe and polyaniline to form the non-precious metal ORR catalyst for full cells [19], however, compared with the Pt/C catalyst, its mass ORR activity is still lower. GDY composes of sp- and sp2-hybridized carbon atoms extending in a 2D plane and reveals to the property of three-dimensional porous materials, which have great potential as alternative carbon support for ORR catalyst.

Under an extremely harsh working condition, the cathode catalysts are under strongly oxidizing conditions: high oxygen concentration, even high potentials (e.g., >1.2 V) for short periods of time. The Pt particles so readily detach from the carbon support that degrades performance during the oxidation process of carbon supports. Furthermore, the size of Pt-based catalysts used in fuel cells is in nanometer scale, but nanoparticles inherently show a strong tendency to agglomerate due to their high specific surface energy. The electrochemical surface area of Pt-based catalysts is going to go down and the general performance of fuel cells will become deterioration, when Pt nanoparticles agglomerate to bigger ones [2, 4]. Therefore, a myriad of studies have focused on solving these issues. The reported approaches involve in improving the carbon support with other species and enhancing the interaction between Pt and the supports. So far, the problem to dissolution and migration of Pt has not been satisfactorily resolved. Hence, it is challenging and highly desired to develop highly stable and efficient ORR catalysts.

Herein, we put forward a facile and effective strategy to encapsulate Pd particles in porous carbon/graphdiyne as a highly stable ORR electrocatalysts (CN_x-Pd@GDY) derived from polyaniline (PANI). Encapsulating Pd particles in porous carbon/graphdiyne with polyaniline (PANI) can not only effectively prevent the Pd nanocrystals from detachment, dissolution, migration, and aggregation during accelerated durability tests or heat-treatment at 900°C, but preserve good electron transfer because the graphdiyne possesses characteristics of three-dimensional porous materials. The interaction between the Pd nanocrystals and the encapsulating PANI shells was found in the prepared catalyst, which markedly contributes to the improvement in catalytic activity and stability. As a result, the CN_x-Pd@GDY catalyst exhibited excellent durability and sufficient ORR catalytic activity.

2. EXPERIMENTAL

First, synthesis of graphdiyne (GDY): GDY was synthesized on the surface of copper via a cross-coupling reaction using $C_{18}H_6$ (hexaethynylbenzene Aladdin Chemical Co.Ltd) as the precursor. In brief, the monomer of $C_{18}H_6$ as new synthesized in good yield (62%) by the addition of $C_{16}H_{36}FN$ (tetrabutylammonium fluoride) to a C_4H_8O (tetrahydrofuran) solution of $C_{36}H_{54}Si_6$ (hexakis [(trimethylsil-yl)-ethynyl] benzene) for 10 min at 8 °C. GDY was successfully grown on the surface of the copper foil in the presence of pyridine by across coupling reaction of the monomer of $C_{18}H_6$ for 72 h at 60 °C under a nitrogen atmosphere. In the process of forming GDY, the copper foil was not only the catalyst for the cross-coupling reaction, but also the substrate for growing the GDY forming. The GDY was then removed from the copper foil ultrasonically and washed in turn with acetone, DMF, 3 mol l^{-1} HCl, 3 mol l^{-1} aqueous NaOH, water and ethanol. After drying under vacuum, the obtained GDY was used as the raw material to synthesize the as-prepared electrocatalysts. The specific experimental procedures of GDY synthesis are detailedly indicated in these reported papers[20].

Synthesis of CN_x-Pd@GDY is as follows. First, 20 mg GDY and 19 mg dipotassium hexachloropalladate (K_2PdCl_6, Aladdin Chemical Co.Ltd) was uniformly dispersed in 30 ml deionized water, assuring the mass ratio of Pd is 20 wt.%. Secondly, 0.1 g of C_6H_7N (aniline purchased from Chongqing Chemical Co.Ltd.) was added into above suspension with stirring for 30 min, and then 1.0 g of $(NH_4)_2S_2O_8$ ammonium peroxydisulfate (APS) as an oxidizing agent was subsequently introduced and controlled the condition to PH = 2 by 0.5 mol l^{-1} HCl solution. The polymerization was performed with vigorous stirring for 24 h at 25 °C to promote the formation of encapsulating Pd particles on GDY surface with polyaniline (PANI). After doing this, the mixture was directly dried under a vacuum at 80 °C for 12 h to produce the samples. Finally the sample was produced at 900 °C for 2 h under N_2 protection to obtain GDY-based catalysts (CN_x-Pd@GDY). The allotropes of carbon (Vulcan XC-72R carbon black) were used to produce the CN_x-Pd@CB catalyst in the same way.

Catalyst characterization: Field-emission scanning electron microscopy (FE-SEM) images were obtained by Hitachi UHR S4800 (Japan). High-resolution transmission electron microscopy (HR-TEM) was carried out on FEI Tecnai F30 instrument and acceleration voltage is 300 kV. X-ray photoelectron spectroscopy (XPS) analysis was performed on Axis Ultra (Kratos Analytical Ltd.).

Electrochemical tests: All the electrochemical ORR tests were obtained on a Zahner Zennium-E electrochemical workstation (ZAHNER Instrument Inc., Germany) with a standard three-electrode electrochemical cell at room temperature. The cell consisted of a glass carbon rotation disk electrode (GC-RDE, 4 mm in diameter, American Pine Instruments), an saturated calomel (SCE) reference electrode, and a platinum foil counter electrode. The fabrication of working electrode was performed by a surface-coating method. Typically, 1 mg of the prepared catalysts and 10 μL of Nafion solution (5.0 wt.% from Aldrich) were well dispersed in 90 μL deionized water. 5.0 ml of 10 mg ml^{-1} dispersion was dropwise added onto the surface of GC-RDE and then dried at room temperature, resulting in the total mass loading of ca. 50 mg. A commercial Pt/C catalyst (20 wt% Pt, E-ETK) on GC-RDE was obtained according to the same procedure described above, but its mass loading was kept at ca. 35 mg. All potentials versus SCE in this study are transferred to the reversible hydrogen electrode (RHE). For the ORR tests, cyclic voltammetry (CV) and linear sweep voltammetry (LSV) measurements were

performed in O_2-saturated 0.1 mol l^{-1} KOH solution by sweeping the potential over the potential range of 1.2 to 0.2 V at the electrode rotated at 500, 800, 1100, 1600, 2000, 2500 and 3600 rpm, respectively.

The electron transfer number (*n*) was calculated from the Koutecky-Levich equation:

$$1/j_d = 1/j_k + 1/B\omega^{1/2}$$

$$B = 0.62nFC_O D_O^{2/3} v^{-1/6} \omega^{1/2}$$

where F is the Faraday constant (96485 C mol^{-1}), C_O is the O_2 saturation concentration in the KOH electrolyte (1.2×10^{-6} mol cm^{-3}), D_O is the O_2 diffusion coefficient in the KOH electrolyte (1.9×10^{-5} cm^2 s^{-1}), n is the kinetic viscosity of the KOH electrolyte (0.01 cm^2 s^{-1}), and u is the elect rode rotation speed, and 0.62 is a constant when the rotation rate is expressed in rpm.

3. RESULTS AND DISCUSSION

The morphology of CN_x-Pd@GDY synthesized under optimum experimental conditions were characterized by the scanning electron microscope (SEM) and the transmission electron microscopy (TEM). It can be seen from the SEM image (Figure 1a) that the Pd nanoparticles effectively are encapsulated in porous carbon/graphdiyne. Figure 1b reveals the high dispersity of Pd nanoparticles in porous carbon/graphdiyne. The TEM images (Figure 1c) may shows the interaction between the Pd nanocrystals and the encapsulating PANI shells in the catalyst, which is a key factor in improving catalyst activity and stability.

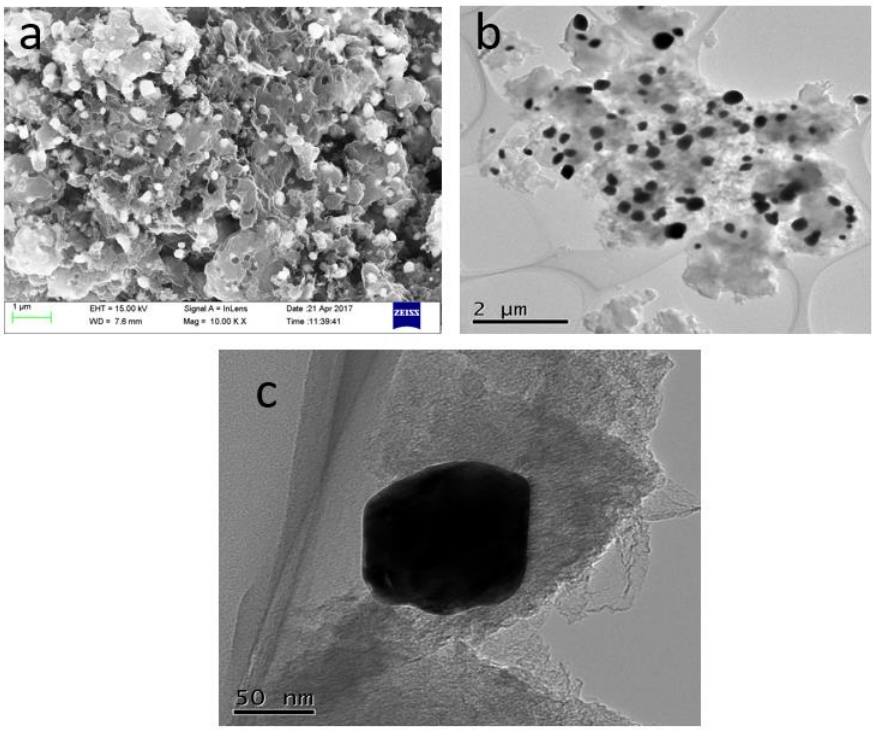

Figure 1. (a,b) SEM and (c) HR-TEM images of the CN_x-Pd@GDY electrocatalyst.

The XPS (X-ray photoelectron spectroscopy) analysis were applied to further characterize the element compositions of CN_x-Pd@GDY. As revealed in Figure 2a, the XPS survey spectra reveal the

successful incorporation of nitrogen atoms into the graphite structure of electrocatalyst, and further suggest that the doped nitrogen is integrated into the CN_x-Pd@GDY sample in terms of pyrrolic N (400.3 eV), graphitic N (401.5 eV) in the high-resolution N1s XPS spectra of CN_x-Pd@GDY (Figure 2c). The presence of Pd atoms in the form of Pd groups was revealed in the Figure 2b, which is owing to $Pd3d_{2/5}$ at 335.25eV, $Pd3d_{2/3}$ at 336.4 eV, $Pd3d_{2/3}$ at 340.65 eV [21-23].

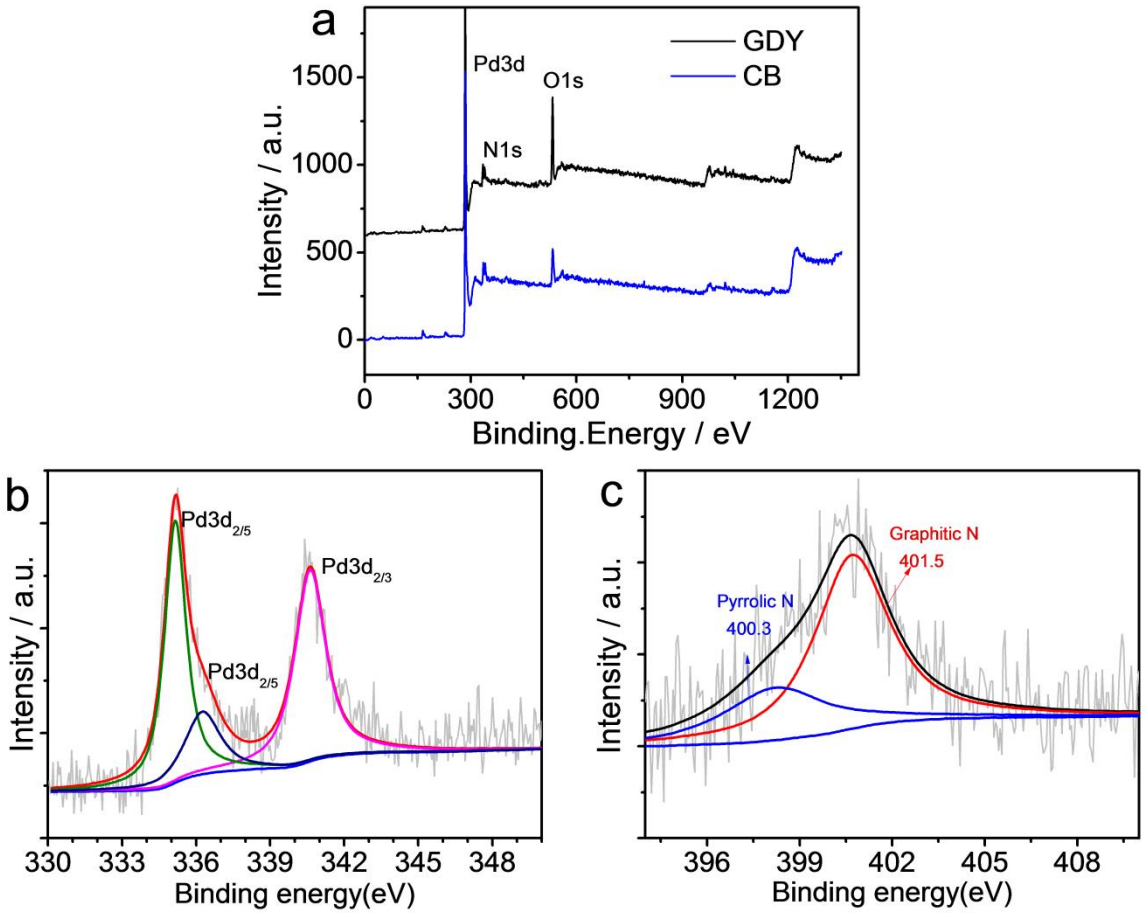

Figure 2. (a) XPS spectra of CN_x-Pd@GDY; (b) High-resolution Pd XPS spectra of CN_x-Pd@GDY; (c) High-resolution N1s XPS spectra of CN_x-Pd@GDY.

To gain insights into how the nitrogen-doped carbon protecting layers or different carbon supports affect the ORR catalytic performance of the prepared catalysts, we have studied the cyclic voltammograms (CV) and linear sweep voltammetry (LSV) experiments in 0.1 mol l^{-1} KOH solution saturated by O_2 or N_2 on the CN_x-Pd@GDY, CN_x-Pd@CB and Pt/C catalysts (20 wt % Pt) for comparison. The CV curves of the samples are exhibited in Figure 3a-c. The catalyzed electrode made with the CN_x-Pd@GDY catalyst shows a little lower ORR catalytic activity with a positive cathodic onset potential (E_p= 0.96 V) compared to the commercial 20 wt % Pt/C catalyst (E_p = 1.05 V). Interestingly, the limited current density of all prepared catalysts can reach to ~5.2 mA cm^{-2}, approaching to that of the Pt/C catalyst, as shown in Figure 3d. Furthermore, the difference of peak potential between

CN_x-Pd@GDY and Pt/C catalyst is only about 70 mV, but the peak potential difference between CN_x-Pd@GB and Pt/C is up to ~160 mV.

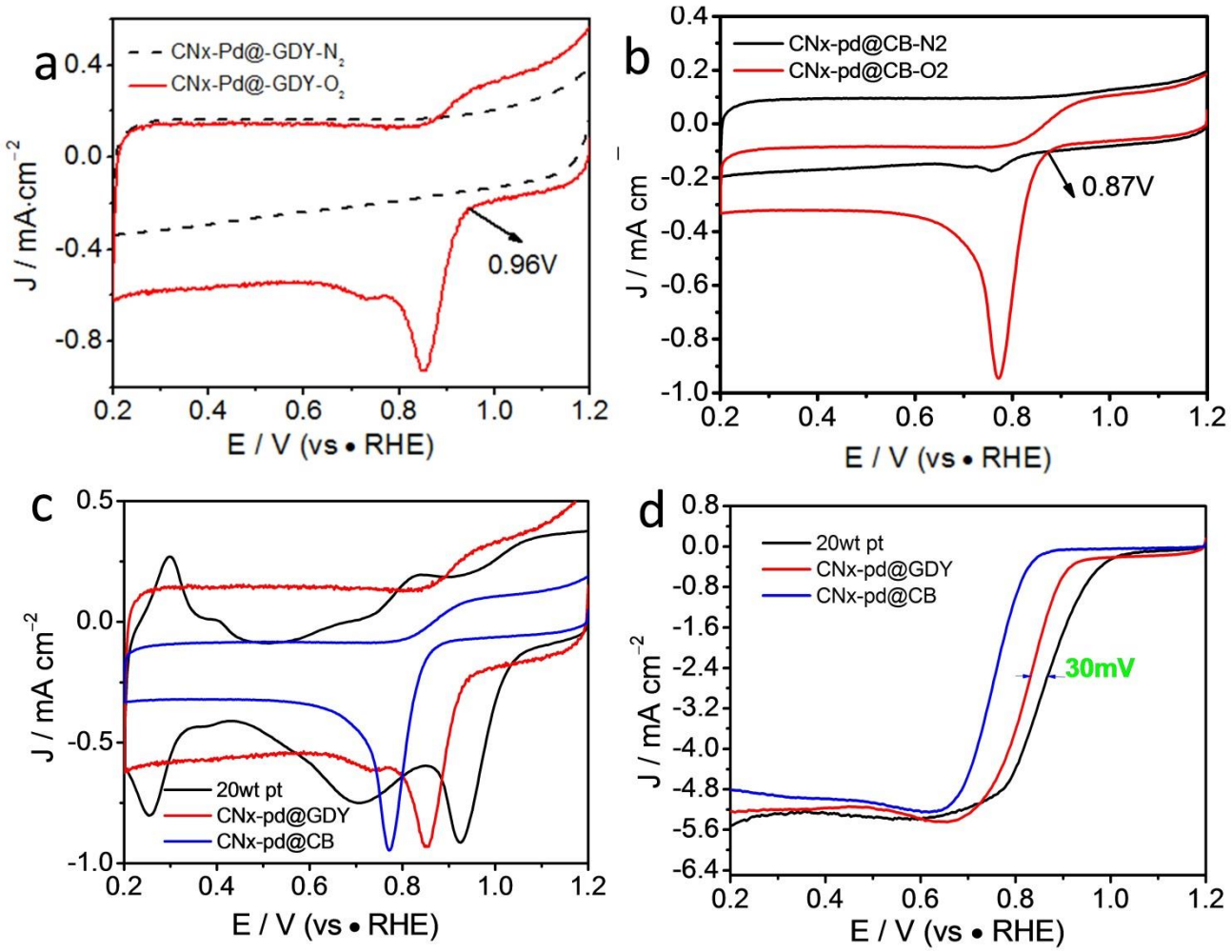

Figure 3. CV (a) and LSV (b) curves of CN_x-Pd@GDY, CN_x-Pd@CB, 20 wt % Pt/C, in 0.1 mol l^{-1} KOH solution saturated by O_2; (c-d) CV of CN_x-Pd@GDY and CN_x-Pd@GB in N_2 or O_2-saturated 0.1 mol l^{-1} KOH solution.

Although the peak potential of CN_x-Pd@GDY is lower than that of the 20 wt.% Pt/C catalyst, however a negligible change in the peak potential is observed at the CN_x-Pd@GDY compared to the apparent shift observed at the CN_x-Pd@GB catalyst, which suggests better ORR electrocatalytic activity of CN_x-Pd@GDY in KOH solution. To further investigate the ORR activity of the samples, linear sweep voltammetry (LSV) curves of CN_x-Pd@GDY, CN_x-Pd@GB and 20 wt.% Pt/C catalysts were measured in O_2-saturated 0.1 mol l^{-1} KOH solution at a rotation rate of 1600 rpm (Figure 3d). The half-wave potential ($E_{1/2}$) is about 0.83, 0.75, and 0.86 V *vs.* RHE, corresponding to CN_x-Pd@GDY, CN_x-Pd@GB and 20 wt.% Pt/C catalyst, respectively. The difference of $E_{1/2}$ between CN_x-Pd@GDY and Pt/C is only ~30mV, implying that the ORR activity of CN_x-Pd@GDY is still lower than that of the Pt/C catalyst in the KOH solution, but the limited diffusion current density (j_d) of CN_x-Pd@GDY is almost identical to

that of the Pt/C catalyst, indicating a relatively higher ORR activity of CN_x-Pd@GDY compared to CN_x-Pd@CB .

The rotating disk electrode voltammetry was used to investigate the ORR activity and ORR mechasiom of CN_x-Pd@GDY and CN_x -Pd@GB in O_2-saturated 0.1 M KOH solution. As shown in Figure 3(a and b), it should be noted that the ORR onset potentials of 0.96 and 0.87 V for CN_x-Pd@GDY and CN_x@GB in an alkaline electrolyte, respectively. These findings indicate that the sample of CN_x-Pd@GDY is better ORR electrocatalytic activity in 0.1 M KOH under the same condition. A comparison of the CV profiles in N_2-saturated electrolyte of the two electrocatalysts reveals the strong reduction peak in the electrolyte saturated with O_2. To further gain insight the ORR kinetics of CN_x-Pd@@GDY, a set of polarization curves for ORR were carefully examined (Figure 4a) at varied rotation speeds in O_2-saturated 0.1 M KOH. We find that the limiting diffusion current density is increased, when the RDE rotation rate is increased. It is reasonable to suggest the current was kinetically controlled. Figure 4b shows the calculated curves of Koutecky−Levich plots, It can be observed that good linearity and near parallelism of the fitting lines. These results clearly indicated that the sample have similar electron transfer numbers for ORR at different potentials and have the first-order reaction kinetics toward the concentration of dissolved oxygen. The electron transfer number of CN_x-Pd@@GDY was calculated to be ~3.8.. We can indentify that a typically mixed two and four-electron reduction pathway ($O_2 + 2H_2O +4e^- \rightarrow 4OH^-$) is proceeded in sample of CN_x-Pd@@GDY catalyst, which is extraordinarily similar to ORR catalyzed by a Pt/C catalyst in the KOH solution. We also measured the RDE curves of CN_x-Pd@@GB at different rotation rates speed range from 500 to 3600 rpm in Figure 4c. It should be noted that the ORR current density increases with the improvement of rotation rate. Seven j values corresponding to the potential range from 0.2 to 0.6 V on every LSV curve were taken. As shown in Figure 4d, the good linear relationship of Koutecky–Levich plots exhibits the first-order ORR kinetics regarding dissolved- oxygen concentration. The ORR electron transfer number, which is a significant parameter in ORR electrocatalysis, is calculated to be about 4.0 at the potential range of 0.2-0.6 V for CN_x-Pd@GB according to the slopes of Koutecky-Levich plots. This phenomena indicate that CN_x-Pd@GDY serves as a single four-electron transfer pathways, however, the four-electron transfer process mainly produces the water. Combined the ORR activity and ORR mechanism, it can be found that the CN_x-Pd @GDY has reasonably indicate a great potential as a new catalysts for ORR instead of the commercial Pt-based catalyst [24].

The stability of CN_x-Pd@GDY electrocatalyst: To further understand the effect of the CN_x layer in the designed CN_x-Pd@GDY catalyst effect on effectively stabilizing Pd nanocrystals, the CV accelerated aging tests (AAT) for CN_x-Pd@GDY and 20wt % Pt/C were performed in O_2-saturated 0.1 mol l^{-1} KOH solution. As can be found, for CV curves and ORR polarization curves (Figure 5a-b), the CN_x-Pd@GDY catalyst exhibits the negligible change of ORR catalytic activity (Figure 3a) while the ORR peak current density underwents a slight loss after the AAT process.

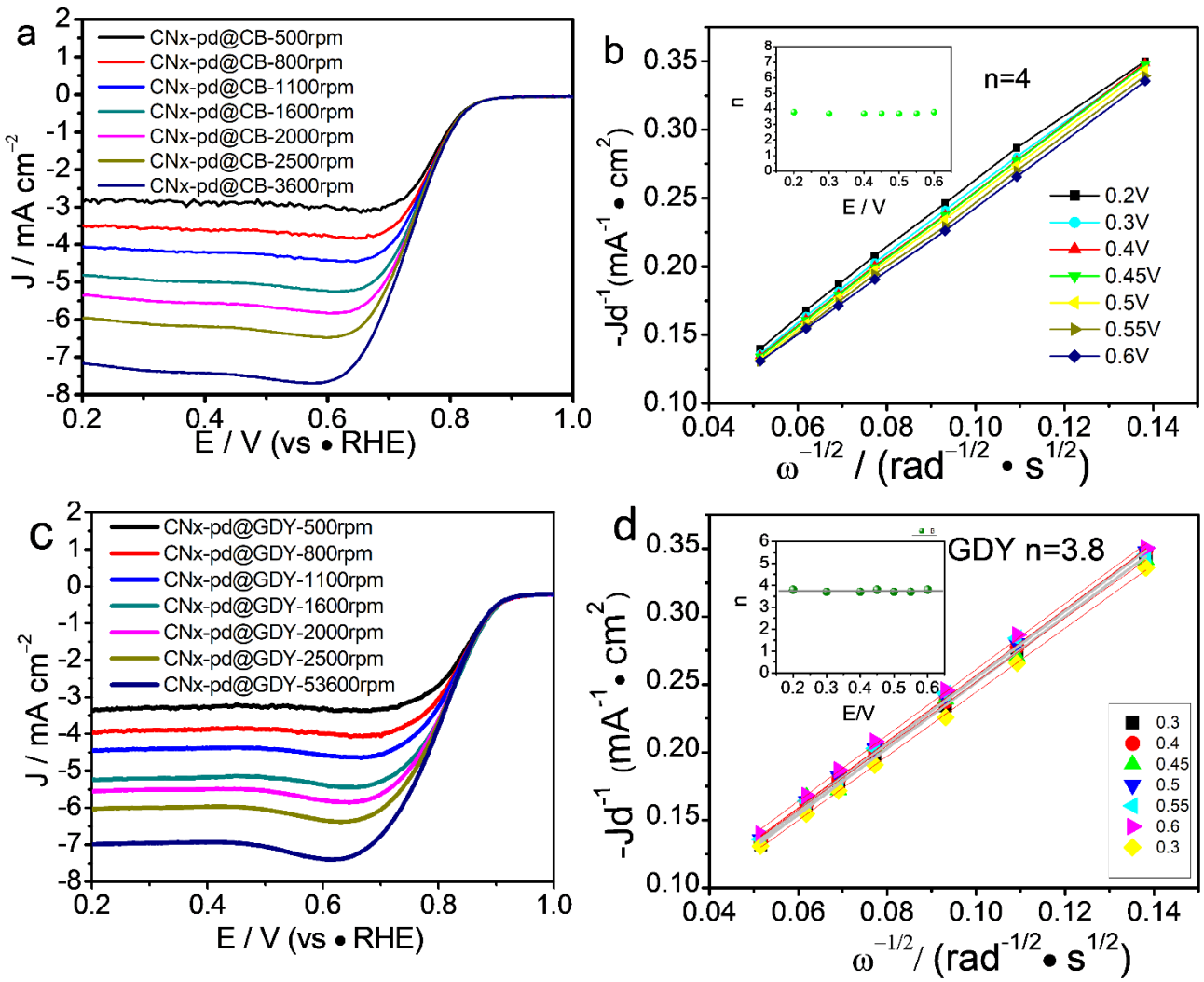

Figure 4. LSV of CN_x-Pd@CB (a) and CN_x-Pd @GDY (c) in O_2-saturated KOH solution at different rotation rates; Koutecky-Levich plots of CN_x-Pd @GB (b) and CN_x-Pd@GDY (d) derived from RDE data.

However, it can be observed that the ORR limited current density is clearly decreased in the LSV curves after the AAT. Besides, the LSV curve shows a negative shift about 25 mV in half-wave potential while the ORR onset potential has negative shift about 10 mV before and after AAT. However, according to the CV and LSV curve of CN_x-Pd@GB, it shows a little positive shift on half-wave potential after CV for 5000 cycles in Figure 5c-d. According to the LSV curve of Pt/C (20 wt%), it is showed a large negative shift on half-wave potential after CV for 5000 cycles [29]. It is worth noting that the ORR performance of both CN_x-Pd@GB and CN_x-Pd@GDY for ORR catalysis obtained in this study is much higher than previous studies and is comparable to the some carbon-based electrocatalysts in previous reports of onset potential, half-wave potential, electron transfer number and current density [25-28]. The long-term stability of CN_x-Pd@GDY demonstratesI the excellent durability in the alkaline solution. It is a novel catalyst and suitable for application in the alkaline ORR electrocatalysis.

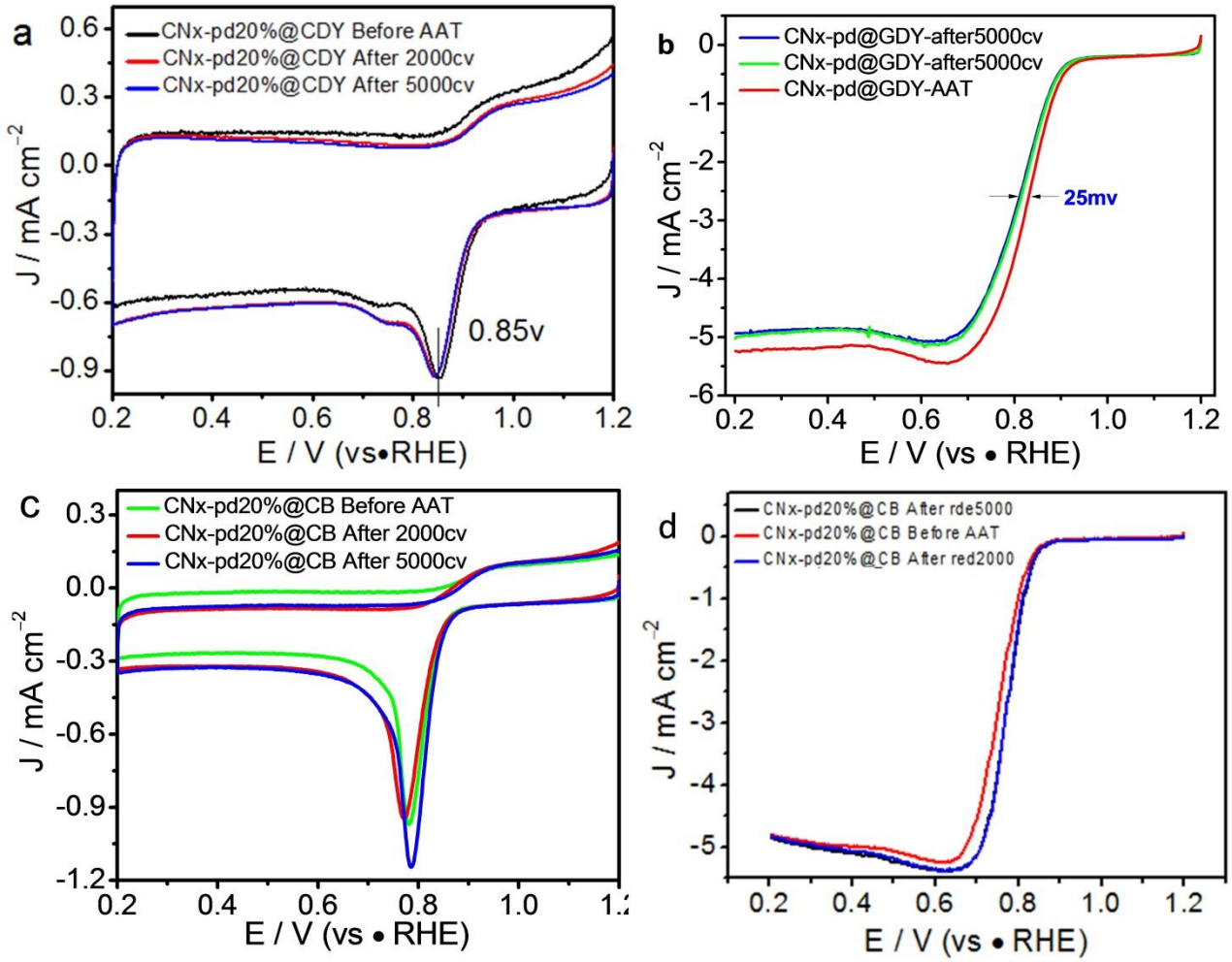

Figure 5. (a) CV and (b) LSV curves of CN_x-Pd@GDY before and after AAT in 0.1 mol l^{-1} KOH solution saturated by O_2. (c) CV and (d) LSV curves of CN_x-Pd@GB before and after AAT in 0.1 mol l^{-1} KOH solution saturated by O_2.

4. CONCLUSIONS

In summary, we have developed a facile and rapid approach to encapsulate Pd nanoparticles in porous carbon/graphdiyne surface as a highly stable electrocatalyst derived from polyaniline. When the accelerated durability tests or heat-treatment at 900 °C, encapsulating Pd nanoparticles in polyaniline-derived porous carbon/graphdiyne can not only effectively prevent the Pt nanocrystals from detachment, dissolution, migration and aggregation, but also preserve good electron transfer because the graphdiyne possesses the characteristics of three-dimensional materials. The interaction between the Pd nanocrystals and the encapsulating PANI shells is found in the catalyst, which markedly contributes to the improvement in ORR catalytic activity and stability. These excellent catalytic characteristics have reasonably indicated a great potential as a novel catalyst for ORR instead of commercial Pt-based catalysts.

A LIST OF ABBREVIATIONS USED IN THE MANUSCRIPT:

GD: graphdiyne
CN_x-Pd@GDY: Pd nanoparticles anchored on nitrogen-doped graphdiyne
PANI: polyaniline
PEMFCs: proton exchange membrane fuel cells
ORR: oxygen reduction reaction
Pt/C: platinum/carbon catalyst
E_p: peak potential
E_{ORR}: onset potential
$E_{1/2}$: half-wave potential
GC: glassy carbon
RRDE: rotation ring-disk electrode
RDE: rotation disk electrode
RHE: reversible hydrogen electrode
LSV: linear sweep voltammetry
CV: cyclic voltammetry
AAT: accelerated aging test
XPS: X-ray photoelectron spectroscopy
FE-SEM: field-emission scanning electron microscopy
HR-TEM: high-resolution transmission electron microscopy

ACKNOWLEDGEMENTS
We gratefully thank Zhongli Luo, Wenli Liao and Jiahong He for helpful discussions and performing some characterization experiments.

FUNDING
This work was financially supported by the National Natural Science Fundation of China (NSFC 21805024), the Basic and Frontier Research Program of Chongqing Municipality (cstc2018jcyjAX0461, cstc2015jcyjA50032), the Scientific and Technological Research Program of Chongqing Municipal Education Commission (KJ1711289, KJ1711285, KJ1501118), the Natural Science Foundation of Yongchuan Science and Technology Commission of Chongqing (Ycstc2016nc6001, Ycsts2018nb1402), the Scientific Research Program of Chongqing University of Arts and Sciences (P2016XC07, 2017YXC51), the Open Project of Engineering Research Center of New Energy Storage Devices and Applications of Chongqing Municipality (KF20170201), and the Innovation Team Project of Chongqing Municipal Education Commission (CXTDX201601037).

AUTHORS' CONTRIBUTIONS
Yanrong Li and Yao Liu carried out the electrochemical experiments and wrote the manuscript. Jin Zhang and Jiaqiang Li prepared the samples and performed the characterizations. Chaozhong Guo,

Zhongbin Li and Jinbiao Wang provided the idea for this work and revised the manuscript. All authors read and approved the final manuscript.

ETHICS APPROVAL AND CONSENT TO PARTICIPATE
Not applicable.

COMPETING INTERESTS
The authors declare that they have no competing interests.

References

1. S. Bai, C. Wang, W. Jiang, N. Du, J. Li, J. Du, R. Long, Z. Li and Y. Xiong, *Nano Res.*, 8 (2015) 2789.
2. B.Y. Xia, Y. Yan, N. Li, H.B. Wu, X.W. Lou and X. Wang, *Nat. Energy*, 1 (2016) 15006.
3. Y. Zheng, Y. Jiao, Y. Zhu, Q. Cai, A. Vasileff, L.H. Li, Y. Han, Y. Chen and S.-Z. Qiao, *J. Am. Chem. Soc.*, 139 (2017) 3336.
4. K. Xu, H. Ding, K. Jia, X. Lu, P. Chen, T. Zhou, H. Cheng, S. Liu, C. Wu and Y. Xie, *Angew. Chem. Int. Ed.*, 55 (2015) 1710.
5. C. Zhang, W. Sandorf and Z. Peng, *ACS Catalysis*, 5 (2015) 2296.
6. C. Zhang, S.Y. Hwang, A. Trout and Z. Peng, *J. Am. Chem. Soc.*, 136 (2014) 7805.
7. H. Yang, H. Li, H. Wang, S. Ji, J. Key and R. Wang, *J. Am. Chem. Soc.*, 161 (2014) F795.
8. G. Wu, K.L. More, C.M. Johnston and P. Zelenay, *Science*, 332 (2011) 443.
9. C. Guo, B. Wen, W. Liao, Z. Li, L. Sun, C. Wang, Y. Wu, J. Chen, Y. Nie, J. Liao and C. Chen, *J. Alloys Compd.*, 686 (2016) 874.
10. J. Zhou, X. Gao, R. Liu, Z. Xie, J. Yang, S. Zhang, G. Zhang, H. Liu, Y. Li, J. Zhang and Z. Liu, *J. Am. Chem. Soc.*, 137 (2015) 7596.
11. R.H. Baughman, H. Eckhardt and M. Kertesz, *J. Chem. Phys.*, 87 (1987) 6687.
12. G. Li, Y. Li, H. Liu, Y. Guo, Y. Li and D. Zhu, *Chem. Commun.*, 46 (2010) 3256.
13. W.B. Wan, C. Brand Stephen, J. Pak Joshua and M. Haley Michael, *Chem.-Eur. J.*, 6 (2000) 2044.
14. N. Yang, Y. Liu, H. Wen, Z. Tang, H. Zhao, Y. Li and D. Wang, *ACS Nano*, 7 (2013) 1504.
15. S. Zhang, H. Liu, C. Huang, G. Cui and Y. Li, *Chem. Commun.*, 51 (2015) 1834.
16. K. Krishnamoorthy, S. Thangavel, J. Chelora Veetil, N. Raju, G. Venugopal and S.J. Kim, *Int. J. Hydrogen Energ.*, 41 (2016) 1672.
17. Z. Jin, Q. Zhou, Y. Chen, P. Mao, H. Li, H. Liu, J. Wang and Y. Li, *Adv. Mater.*, 28 (2016) 3697.
18. X. Gao, J. Zhou, R. Du, Z. Xie, S. Deng, R. Liu, Z. Liu and J. Zhang, *Adv. Mater.*, 28 (2015) 168.
19. Y. Li, C. Guo, J. Li, W. Liao, Z. Li, J. Zhang and C. Chen, *Carbon*, 119 (2017) 201.
20. G. Li, Y. Li, H. Liu, Y. Guo, Y. Li and D. Zhu, *Chem. Commun.*, 46 (2010) 3256.
21. W. Ding, Z. Wei, S. Chen, X. Qi, T. Yang, J. Hu, D. Wang, L.-J. Wan, F. Alvi Shahnaz and L. Li, *Angew. Chem.*, 125 (2013) 11971.
22. J.R. Kitchin, J.K. Nørskov, M.A. Barteau and J.G. Chen , *Phys. Rev. Lett.*, 93 (2004)156801.
23. P. Nowicki, R. Pietrzak and H. Wachowska, *Energ. Fuels*, 24 (2010) 1197.
24. Y. Jiao, Y. Zheng, M. Jaroniec and S.Z. Qiao, *J. Am. Chem. Soc.*, 136 (2014) 4394.
25. H. Wu, C. Guo, J. Li, Z. Ma, Q. Feng and C. Chen, *Int. J. Hydrogen Energ.*, 41 (2016) 20494.
26. J. Zheng, C. Guo, C. Chen, M. Fan, J. Gong, Y. Zhang, T. Zhao, Y. Sun, X. Xu, M. Li, R. Wang, Z. Luo and C. Chen, *Electrochim. Acta*, 168 (2015) 386.
27. C. Guo, W. Liao and C. Chen, *J Power Sources*, 269 (2014) 841.
28. D. Geng, Y. Chen, Y. Chen, Y. Li, R. Li, X. Sun, S. Ye and S. Knight, *Energ. Environ. Sci.*, 4 (2011)

760.
29. C. Guo, Y. Li, W. Liao, Y. Liu, Z. Li, L. Sun, C. Chen,. J. Zhang, Y. Si and L. Li, *J. Mater. Chem. A*, 6 (2018) 13050.